International Journal of Numerical Modelling: Electronic Networks, Devices and Fields

WILEY

RESEARCH ARTICLE OPEN ACCESS

An Affine Linear Solution of the Nonlinear Inverse Power Flow Problem in Resistive Networks

Martin Wachs[1,2] | Miriam Primbs[1]

[1]Institute of Natural Sciences, University of Applied Sciences Ruhr West, Mülheim, Germany | [2]General and Theoretical Electrical Engineering (ATE), University of Duisburg-Essen, and Center for Nanointegration Duisburg-Essen (CENIDE), Duisburg, Germany

Correspondence: Martin Wachs (martin.wachs@hs-ruhrwest.de)

Received: 10 January 2025 | **Accepted:** 3 February 2025

Funding: This work was supported by the Ministry of Culture and Science of the Federal State North Rhine-Westphalia (005-2105-0047).

Keywords: algebraic/geometric methods | electromagnetic tomography | inverse power flow problem

ABSTRACT

In the analysis of linear electrical networks, an inverse problem can be inferring all edge impedances only from known external voltage sources and measured resulting edge currents. Given all external edge voltages $\boldsymbol{u}_{\text{ext}}$ and all resulting edge currents $\boldsymbol{i}$, we present a new calculation method for the edge resistances $\boldsymbol{R}$, with the assumption that the reactance is everywhere zero (e.g., a resistive network). Our considerations are based on affine subspaces and their intersection. We show, that in case of having a sequence of $l \geq 3$ measurements $(\boldsymbol{u}_{\text{ext}_1}, \boldsymbol{i}_1), \ \ldots, (\boldsymbol{u}_{\text{ext}_l}, \boldsymbol{i}_l)$, we can calculate $\boldsymbol{R}$ uniquely in every such network. For a sufficiently large but still small cuboid grid, we can reduce the number of needed measurements to 2.

1 | Introduction

In frameworks such as network theory and associated inverse problems like electrical impedance tomography (EIT), among others, determining impedances from current measurements represents a well-known nonlinear inverse problem. The theoretical approach presented here is rooted in network theory, but is also applicable to solving the inverse problem in tomographic contexts when a network model is employed for the forward problem. It uses a small number of 2 or 3 measurements to calculate the inverse problem.

We will give a brief review of related work dealing with impedance reconstruction. In network theory, a solution to the inverse problem is given in the framework of the inverse power flow problem [1]. However, the required number of measurements is at least equal to the number of nodes inside the network. Another approach with only two measurements for a three-node network section is given in [2]. But still, there is no calculation given for larger networks. In tomographic applications such as magnetic resonance EIT (MREIT), it has been demonstrated [3] that the inverse problem is not unique when only a single current measurement is available. Additionally, it was shown that, in a special case, two measurements can uniquely determine the solution to the inverse problem. Similar results have been reported in [4–6]. However, since EIT is based on conservative current densities, these findings cannot be extended to inverse problems involving eddy currents, as in magnetic induction tomography (MIT). An iterative method for the MIT framework is presented in [7], where two measurements are sufficient to solve the inverse problem in two-dimensional (2D) and three-dimensional (3D). However, this method is less accurate and general than the approach under consideration here.

This paper presents a novel method for arbitrary networks, assuming a resistive network model, which is based on the intersection of affine subspaces. It generally requires at most three measurements and only two measurements for most 3D

settings. Further, it achieves an exact solution for noiseless data. However, it is also fairly stable for noisy data.

The paper is outlined as follows: In the first section, we mathematically introduce the underlying forward problem. In the second section, we show how to calculate all possible solutions $\boldsymbol{R}$ for the electric resistances from a single measurement of external edge voltages $\boldsymbol{u}_{\text{ext}}$ and resulting total edge currents $\boldsymbol{i}$. After that, we show how a sequence of measurements of edge voltages and resulting edge currents provide a unique solution to the inverse problem in at most three steps. Further, we show that in almost all 3D-cuboid settings, only two measurements are needed. Finally, we discuss how the algorithm performs under the effect of measurement errors or noisy data and we will show an example coming from the MIT setting.

2 | The Forward Problem

Since the solution presented in this paper is limited to resistive networks, the forward problem is also restricted to a resistive network model. Each edge in the network can contain a voltage source with a fixed voltage and a resistance strictly greater than 0. The resulting voltage across an entire edge depends on both the voltage source and the resistance, and consequently, on the overall network configuration. Let us consider a network with n nodes and m edges. In the forward problem, the vector of external edge voltages, $\boldsymbol{u}_{\text{ext}} \in \mathbb{R}^m$, and the diagonal resistance matrix, $\boldsymbol{R} = \text{diag}\left(R_i\right)_{i=1}^{m}$ are given. We assume $R_i > 0\Omega$ for all edges $i \in \{1, \ldots, m\}$. Using these, the resulting voltage across each edge is first calculated, followed by the determination of the total edge currents, $\boldsymbol{i} \in \mathbb{R}^m$. This can be done as follows using nodal analysis [8]. We denote by $\boldsymbol{N} \in \mathbb{R}^{n\times m}$ the node edge incidence matrix and by $\boldsymbol{Y} \in \mathbb{R}^{n\times n}$ the corresponding nodal admittance matrix, defined by

$$\boldsymbol{Y} = \boldsymbol{N} \cdot \boldsymbol{R}^{-1} \cdot \boldsymbol{N}^T \tag{1}$$

With $\boldsymbol{u}_{\text{ext}} \in \mathbb{R}^m$ being the vector of external edge voltages, we first get the nodal potential vector $\phi \in \mathbb{R}^n$ as a unique solution of

$$\boldsymbol{Y} \cdot \phi = -\boldsymbol{N} \cdot \boldsymbol{R}^{-1} \cdot \boldsymbol{u}_{\text{ext}}. \tag{2}$$

Here, the uniqueness is ensured by choosing an arbitrary node having zero potential. In this paper, we choose the node number n as the one with zero node potential. Using ϕ, we further get the edge currents by evaluating

$$\boldsymbol{i} = \boldsymbol{i}\left(\boldsymbol{R}, \boldsymbol{u}_{\text{ext}}\right) = \boldsymbol{R}^{-1} \cdot \left(\boldsymbol{u}_{\text{ext}} + \boldsymbol{N}^T \cdot \phi\right). \tag{3}$$

Remark 1. The forward problem $\boldsymbol{i}\left(\boldsymbol{R}, \boldsymbol{u}_{\text{ext}}\right)$ is nonlinear in $\boldsymbol{R}$, but linear in $\boldsymbol{u}_{\text{ext}}$.

3 | The Inverse Problem

The nonlinear inverse problem, we consider here, is to determine the edge resistance in $\boldsymbol{R}$ based on a sequence $\left(\boldsymbol{u}_{\text{ext}_j}, \boldsymbol{i}_j\right)$ of external edge voltages and the related resulting total edge currents. Given a single pair $\left(\boldsymbol{u}_{\text{ext}}, \boldsymbol{i}\right)$ of this type, the task is to find the set of all diagonal matrices $\boldsymbol{R}$, such that (2) and (3) hold. First, we show how to determine this set, which turns out to be always an affine subspace in the vector space of all diagonal matrices of dimension m. Taking into account a sequence $\left(\boldsymbol{u}_{\text{ext}_j}, \boldsymbol{i}_j\right)$ of such pairs, we subsequently show how to derive a unique solution by computing the intersection of all corresponding affine subspaces.

There is one assumption to the network we need to make:

Assumption 1. The inverse calculation of the resistances of two resistors in a series connection can never be calculated uniquely. Only the sum can be calculated. So, for every node that has only two edges, we need to delete this node and represent the adjacent edges by one resistance only. Based on this, we can assume, that every node in the network has at least three adjacent edges.

3.1 | Kernel of the Nodal Analysis

Recall that the kernel of the nodal analysis in (3) is the set of all external edge voltages $\boldsymbol{u}_{\text{ext}}$, such that the resulting currents $\boldsymbol{i}$ are $\boldsymbol{0}$A. For n being the number of nodes, it is well known, that the dimension of the kernel is $n-1$ (cp. [8]). In this section, we show that for choosing the node number n to have zero node potential, the first $n-1$ columns of $\boldsymbol{N}^T$ form a basis of the kernel, which is independent of $\boldsymbol{R}$. To correctly represent all physical units, we use the units A for Ampère, V for Volt, and Ω for Ohm in some instances as a factor in the equations.

Definition 1. We define the sink voltage matrix

$$\boldsymbol{U}_{\text{sink}} = \boldsymbol{N}^T \cdot 1\text{V} \in \mathbb{R}^{m\times n}$$

and for any node $k \in \{1, \ldots, n-1\}$, the kth sink voltage vector by

$$\boldsymbol{u}_{\text{sink}}(k) = \boldsymbol{U}_{\text{sink}} \cdot \boldsymbol{e}_k \in \mathbb{R}^m \tag{4}$$

being the kth column vector of $\boldsymbol{U}_{\text{sink}}$. Further, for later use, we define

$$\boldsymbol{U}_{\text{sink,red}} = \left(\boldsymbol{u}_{\text{sink}}(1), \ldots, \boldsymbol{u}_{\text{sink}}(n-1)\right) \in \mathbb{R}^{m\times(n-1)}$$

as the first $n-1$ columns of $\boldsymbol{U}_{\text{sink}}$.

Remark 2. It is well-known (cp. [8]), that the kernel of the nodal analysis is of dimension $n-1$ and that the row rank of $\boldsymbol{N}$ is $n-1$. Further, deleting an arbitrary row of $\boldsymbol{N}$ leads to a matrix of full row rank $n-1$. Deleting the n-th row is equivalent to the choice of the zero potential node being the node number n. Thus, $\boldsymbol{U}_{\text{sink,red}}$ is of full column rank $n-1$, and the column vectors are linearly independent and span a $(n-1)$-dimensional space of $\mathbb{R}^m$. This space is now to be shown to be the kernel of the nodal analysis for node n with zero potential, independent of $\boldsymbol{R}$.

Lemma 1. *Choosing node number n to have zero node potential, the set*

$$\mathcal{U}_{\text{sink}} = \text{span}\{\boldsymbol{u}_{\text{sink}}(k) \mid k \in \{1, \ldots, n-1\}\} \tag{5}$$

is the $(n-1)$*-dimensional kernel of the nodal analysis, where*

$$\{\boldsymbol{u}_{\text{sink}}(k) \mid k \in \{1, \ldots, n-1\}\}$$

is a basis of $\mathcal{U}_{\text{sink}}$ *which is independent of* $\boldsymbol{R}$.

Proof. The dimension statement directly follows from Remark 2. It remains to show that for every vector $\boldsymbol{u}_{\text{ext}} = \boldsymbol{U}_{\text{sink}} \cdot \boldsymbol{a}$ with an arbitrary coefficient vector $\boldsymbol{a} \in \mathbb{R}^n$ with $a_n = 0$ the equation

$$\boldsymbol{i}(\boldsymbol{R}, \boldsymbol{u}_{\text{ext}}) = \boldsymbol{0}\text{A}. \tag{6}$$

holds. Inserting $\boldsymbol{u}_{\text{ext}} = \boldsymbol{U}_{\text{sink}} \cdot \boldsymbol{a}$ in (2) and using (1), we get

$$\boldsymbol{Y} \cdot \boldsymbol{\phi} = -\boldsymbol{N} \cdot \boldsymbol{R}^{-1} \cdot \boldsymbol{U}_{\text{sink}} \cdot \boldsymbol{a} \quad \Leftrightarrow \quad \boldsymbol{Y} \cdot \boldsymbol{\phi} = -\boldsymbol{Y}\boldsymbol{a}\text{V}. \tag{7}$$

The unique solution under the precondition $a_n = 0$ is the trivial solution $\boldsymbol{\phi} = -\boldsymbol{a}$V (cp. [8]). We now set $\boldsymbol{\phi} = -\boldsymbol{a}$V in (3) to receive

$$\boldsymbol{i} = \boldsymbol{R}^{-1} \cdot (\boldsymbol{u}_{\text{ext}} + \boldsymbol{N}^T \cdot (-\boldsymbol{a}\text{V})) = \boldsymbol{R}^{-1} \cdot (\boldsymbol{U}_{\text{sink}} \cdot \boldsymbol{a} - \boldsymbol{N}^T \cdot \boldsymbol{a}\text{V}) = \boldsymbol{0}\text{A}.$$

This means $\mathcal{U}_{\text{sink}}$ is the kernel of the nodal analysis and the set of column vectors of $\boldsymbol{U}_{\text{sink,red}}$ is its basis. Since $\boldsymbol{N}$ is independent of $\boldsymbol{R}$, the basis $\{\boldsymbol{u}_{\text{sink}}(k) \mid k \in \{1, \ldots, n-1\}\}$ is as well. □

3.2 | A Special Mathematical Solution of the Inverse Problem

Given a pair $(\boldsymbol{u}_{\text{ext}}, \boldsymbol{i})$ of external edge voltages and resulting total edge currents, we show that the element-wise quotient $\boldsymbol{u}_{\text{ext}} / \boldsymbol{i}$ is a simple mathematical but potentially non-physical solution of the inverse problem. From now on the quotient of two vectors is always to be considered element-wise. The presence of negative resistance is temporarily accepted.

Lemma 2. *Given a pair* $(\boldsymbol{u}_{\text{ext}}, \boldsymbol{i})$ *and setting* $\boldsymbol{R}(\boldsymbol{u}_{\text{ext}}, \boldsymbol{i}) := \text{diag}(\boldsymbol{u}_{\text{ext}} / \boldsymbol{i})$, *Equation (3) based on (2) is valid. Thus,* $\boldsymbol{R}(\boldsymbol{u}_{\text{ext}}, \boldsymbol{i})$ *is a solution of the inverse problem set by* $(\boldsymbol{u}_{\text{ext}}, \boldsymbol{i})$.

Proof. The resulting currents hold the Kirchhoff's junction rule, that is,

$$\boldsymbol{N} \cdot \boldsymbol{i} = \boldsymbol{0}\text{A}.$$

Thus, entering $\boldsymbol{R}^{-1}(\boldsymbol{u}_{\text{ext}}, \boldsymbol{i}) = \text{diag}(\boldsymbol{i} / \boldsymbol{u}_{\text{ext}})$ in (2), the equation for the determination of the node potential becomes

$$\boldsymbol{Y} \cdot \boldsymbol{\phi} = -\boldsymbol{N} \cdot \text{diag}(\boldsymbol{i} / \boldsymbol{u}_{\text{ext}}) \cdot \boldsymbol{u}_{\text{ext}} = -\boldsymbol{N} \cdot \boldsymbol{i} = \boldsymbol{0}\text{A} \tag{8}$$

and thus the trivial solution $\boldsymbol{\phi} = \boldsymbol{0}$V follows. Using $\boldsymbol{\phi} = \boldsymbol{0}$V in the right side of (3), we get

$$\boldsymbol{R}^{-1}(\boldsymbol{u}_{\text{ext}}, \boldsymbol{i}) \cdot (\boldsymbol{u}_{\text{ext}} + \boldsymbol{N}^T \cdot \boldsymbol{\phi}) = \boldsymbol{R}^{-1}(\boldsymbol{u}_{\text{ext}}, \boldsymbol{i}) \cdot \boldsymbol{u}_{\text{ext}} = \boldsymbol{i}. \tag{9}$$

3.3 | The Solution Set of the Inverse Problem

Based on a given pair $(\boldsymbol{u}_{\text{ext}}, \boldsymbol{i})$ and its related matrix $\boldsymbol{R}(\boldsymbol{u}_{\text{ext}}, \boldsymbol{i}) := \text{diag}(\boldsymbol{u}_{\text{ext}} / \boldsymbol{i})$, we show that the set of all possible solutions $\boldsymbol{R}$ such that (2) and (3) hold, always has the same affine subspace structure.

Lemma 3.

1. *Using the notation from Lemma 2, a diagonal matrix* $\boldsymbol{R}$ *is a solution of the inverse problem set by the pair* $(\boldsymbol{u}_{\text{ext}}, \boldsymbol{i})$ *if and only if*

$$\boldsymbol{R} = \boldsymbol{R}(\boldsymbol{u}_{\text{ext}}, \boldsymbol{i}) + \text{diag}\left(\frac{\boldsymbol{u}_{\text{sink}}}{\boldsymbol{i}}\right) = \text{diag}\left(\frac{\boldsymbol{u}_{\text{ext}} + \boldsymbol{u}_{\text{sink}}}{\boldsymbol{i}}\right) \tag{10}$$

for a $\boldsymbol{u}_{\text{sink}} \in \mathcal{U}_{\text{sink}}$.

2. *The solution set of the inverse problem, given a single pair* $(\boldsymbol{u}, \boldsymbol{i})$, *is the affine subspace*

$$\mathcal{R}(\boldsymbol{u}_{\text{ext}}, \boldsymbol{i}) = \boldsymbol{R}(\boldsymbol{u}_{\text{ext}}, \boldsymbol{i}) + \mathcal{U}_{\text{sink}} / \boldsymbol{i} = \left\{\text{diag}\left(\frac{\boldsymbol{u}_{\text{ext}}}{\boldsymbol{i}} + \frac{\boldsymbol{u}_{\text{sink}}}{\boldsymbol{i}}\right) \mid \boldsymbol{u}_{\text{sink}} \in \mathcal{U}_{\text{sink}}\right\}. \tag{11}$$

Proof. Let $\boldsymbol{R}$ be any diagonal matrix of resistances, not necessarily a solution of the inverse problem set by $(\boldsymbol{u}_{\text{ext}}, \boldsymbol{i})$. Setting $\widetilde{\boldsymbol{u}}_{\text{ext}} = \boldsymbol{R} \cdot \boldsymbol{i}$ we get by Lemma 2 and Remark 1:

$$\boldsymbol{i} =: \boldsymbol{i}(\boldsymbol{R}(\boldsymbol{u}_{\text{ext}}, \boldsymbol{i}), \boldsymbol{u}_{\text{ext}}) = \boldsymbol{i}(\boldsymbol{R}, \widetilde{\boldsymbol{u}}_{\text{ext}}) = \boldsymbol{i}(\boldsymbol{R}, \boldsymbol{u}_{\text{ext}}) + \boldsymbol{i}(\boldsymbol{R}, \widetilde{\boldsymbol{u}}_{\text{ext}} - \boldsymbol{u}_{\text{ext}}) \tag{12}$$

Thus, $\boldsymbol{R}$ is a solution of the inverse problem set by $(\boldsymbol{u}_{\text{ext}}, \boldsymbol{i})$, that is, $\boldsymbol{i} = \boldsymbol{i}(\boldsymbol{R}, \boldsymbol{u}_{\text{ext}})$, if and only if $\boldsymbol{i}(\boldsymbol{R}, \widetilde{\boldsymbol{u}}_{\text{ext}} - \boldsymbol{u}_{\text{ext}}) = \boldsymbol{0}$. Further by Lemma 1 $\widetilde{\boldsymbol{u}}_{\text{ext}} - \boldsymbol{u}_{\text{ext}} \in \ker(\boldsymbol{i}(\boldsymbol{R}, \circ))$ if and only if there exist a $\boldsymbol{u}_{\text{sink}}$ with $\widetilde{\boldsymbol{u}}_{\text{ext}} - \boldsymbol{u}_{\text{ext}} = \boldsymbol{u}_{\text{sink}}$, that is, $\boldsymbol{R} = \text{diag}((\boldsymbol{u}_{\text{ext}} + \boldsymbol{u}_{\text{sink}}) / \boldsymbol{i})$. This proves 1. and therefore automatically 2. □

Remark 3. *Since* $\dim(\mathcal{U}_{\text{sink}}) = n - 1$ *(cp. Lemma 1), we also have*

$$\dim(\mathcal{R}(\boldsymbol{u}_{\text{ext}}, \boldsymbol{i})) = n - 1.$$

3.4 | Finding a Unique Solution

In this section, we show how to find a unique solution to the inverse problem by the intersection of a sequence of affine subspaces. Methods on how to compute those intersections and also criteria on how to guarantee that the result only contains a single element can be found in [9]. We summarize this paper for our problem in the subsequent theorem. For the sake of convenience, we adapt the representation of $\mathcal{R}(\boldsymbol{u}_{\text{ext}}, \boldsymbol{i})$ to the notation used there. Using (4) and (5) and setting $\boldsymbol{s} := \frac{\boldsymbol{u}_{\text{ext}}}{\boldsymbol{i}}$ and $\boldsymbol{A} := (\text{diag}(\boldsymbol{i}))^{-1} \cdot \boldsymbol{U}_{\text{sink,red}}$, we can write

$$\mathcal{R}(\boldsymbol{u}_{\text{ext}}, \boldsymbol{i}) = \mathcal{R}(\boldsymbol{s}, \boldsymbol{A}) = \{\text{diag}(\boldsymbol{s} + \boldsymbol{A} \cdot \boldsymbol{x}) \mid \boldsymbol{x} \in \mathbb{R}^{n-1}\}. \tag{13}$$

A sequence of l measurements with related affine subspaces $\mathscr{R}_k = \mathscr{R}(\boldsymbol{s}_k, \boldsymbol{A}_k)$, $k = 1, \dots, l$, only has a unique solution $\boldsymbol{R}$, if $\cap_{k=1}^{l} \mathscr{R}_k = \{\boldsymbol{R}\}$, that is, the dimension of the intersection is $\mathbf{0}$.

Theorem 1. *Given a sequence of measurements* $(\boldsymbol{u}_{\text{ext}_k}, \boldsymbol{i}_k), k = 1, \dots, l$, *with the corresponding solution sets* $\mathscr{R}_k := \mathscr{R}(\boldsymbol{s}_k, \boldsymbol{A}_k)$, *the solution for* $\boldsymbol{R}$ *can be calculated by solving the equation*

$$\begin{pmatrix} \boldsymbol{A}_1 & \boldsymbol{A}_2 & & & \\ \boldsymbol{A}_1 & & \boldsymbol{A}_3 & & \\ \vdots & & & \ddots & \\ \boldsymbol{A}_1 & & & & \boldsymbol{A}_l \end{pmatrix} \cdot \begin{pmatrix} \boldsymbol{x}_1 \\ \boldsymbol{x}_2 \\ \vdots \\ \boldsymbol{x}_l \end{pmatrix} = \begin{pmatrix} \boldsymbol{s}_2 - \boldsymbol{s}_1 \\ \boldsymbol{s}_3 - \boldsymbol{s}_1 \\ \vdots \\ \boldsymbol{s}_l - \boldsymbol{s}_1 \end{pmatrix}. \tag{14}$$

The solution $(\boldsymbol{x}_1, \dots, \boldsymbol{x}_l)$ *is unique, that is, the dimension of the intersection of the affine subspaces is* 0, *if and only if the matrix in Equation (14) has full column rank. The solution* $\boldsymbol{R}$ *is then calculated by*

$$\boldsymbol{R} = \operatorname{diag}(\boldsymbol{s}_k + \boldsymbol{A}_k \cdot \boldsymbol{x}_k)$$

with an arbitrary $k \in \{1, \dots, l\}$.

Now we calculate the number l that we need at least so that $\boldsymbol{R}$ can be determined uniquely. Therefore, we want the affine subspaces to be maximal independent from each other. This means the intersection of two such subspaces is minimal.

Definition 2.
1. Let $\mathscr{R}_1$ and $\mathscr{R}_2$ be two affine subspaces of a d-dimensional space $\mathscr{R}$. We call the two subspaces maximal independent if the intersection is not empty and of minimal dimension:

$$\dim(\mathscr{R}_1 \cap \mathscr{R}_2) = \max(0, \dim(\mathscr{R}_1) + \dim(\mathscr{R}_2) - \dim(\mathscr{R})).$$

2. We call a sequence of affine subspaces maximal independent, if the intersection of all subspaces is not empty and of minimal dimension.

Now, we can turn to the question of how many measurements we need for a unique determination of the resistances.

Theorem 2. *Given a network with* n *nodes and* m *edges and a sequence of measurements* $(\boldsymbol{u}_{\text{ext}_k}, \boldsymbol{i}_k), k = 1, \dots, l$, *such that the corresponding solution sets* $\mathscr{R}_k := \mathscr{R}(\boldsymbol{u}_{\text{ext}_k}, \boldsymbol{i}_k)$ *are maximal independent, we can show*

$$\dim(\cap_{k=1}^{l} \mathscr{R}_k) = \max(0, l \cdot (n-1) - (l-1) \cdot m). \tag{15}$$

Consequently, the solution for $\boldsymbol{R}$ *is unique if and only if*

$$l \cdot (n-1) - (l-1) \cdot m \leq 0 \tag{16}$$

Proof. We can calculate the dimension of the intersection of two maximal independent subspaces by

$$\dim(\mathscr{R}_1 \cap \mathscr{R}_2) = \max(0, 2(n-1) - m).$$

The dimension of the intersection of three maximal independent subspaces is:

$$\begin{aligned} &\dim(\mathscr{R}_1 \cap \mathscr{R}_2 \cap \mathscr{R}_3) \\ &= \max(0, 2(n-1) - m + (n-1) - m) \\ &= \max(0, 3(n-1) - 2m). \end{aligned}$$

By induction, we get the dimension of the intersection of l maximal independent subspaces

$$\dim(\cap_{k=1}^{l} \mathscr{R}_k) = \max(0, l \cdot (n-1) - (l-1) \cdot m).$$

From the assumption $l \cdot (n-1) - (l-1) \cdot m \leq 0$ we get

$$\dim(\cap_{k=1}^{l} \mathscr{R}_k) = 0. \qquad \square$$

4 | Number of Needed Measurements

In this section, we show that the number of measurements required with the proposed method is very small. For an arbitrary network three and for a cuboid grid network of sufficient but still small size, only two measurements are needed for uniqueness.

4.1 | In General Networks

Theorem 3. *In an arbitrary network we need at most three measurements, with maximal independent solution sets* $\mathscr{R}_1, \mathscr{R}_2, \mathscr{R}_3$, *to get a unique solution for the inverse problem.*

Proof. From Assumption 1, we get that every node has at least three edges. Furthermore, every edge has exactly two nodes. Thus, we have the following inequality for n nodes and m edges:

$$n \leq \frac{2}{3} m$$

We evaluate the Equation (16) from Theorem 2 for $l = 3$ and get

$$\begin{aligned} 3 \cdot (n-1) - 2 \cdot m &\leq 3 \cdot \left(\frac{2}{3} m - 1\right) - 2 \cdot m \\ &= 2m - 3 - 2m = -3 \leq 0, \end{aligned}$$

which proofs

$$\dim(\cap_{k=1}^{3} \mathscr{R}_k) = 0. \qquad \square$$

4.2 | In Cuboid Grids

The inverse power flow problem is a subproblem in various electromagnetic tomographic techniques for biological tissue, such as MIT [10] and EIT [11, 12]. In these cases, the problem is better known as inverse problem of the (reduced) eddy current

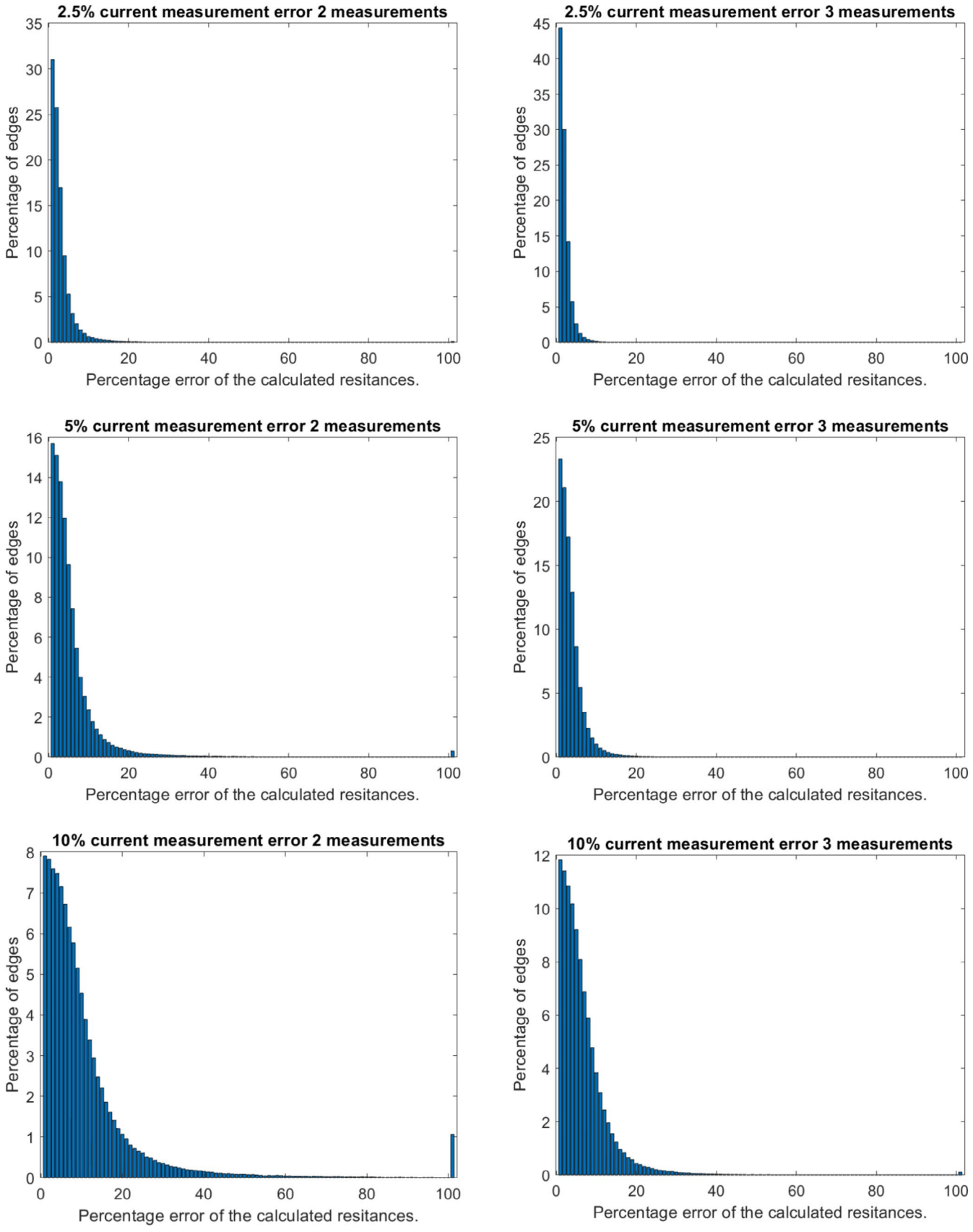

FIGURE 1 | Current measurement error for different percentages for two and three measurements, respectively.

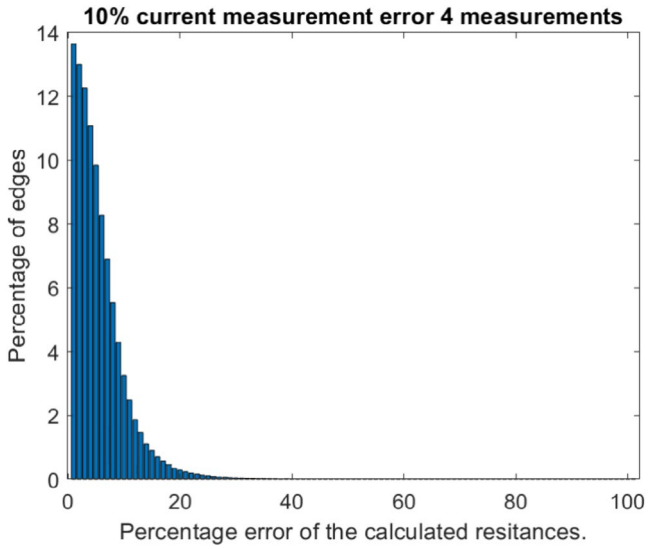

FIGURE 2 | 10% current measurement error with four measurements.

problem. Techniques like the finite integration method [13, 14] and the finite formulation of electromagnetism [15, 16] are often used in these contexts. These methods discretize the Maxwell equations onto lattices and co-lattices, ensuring the integral form of the Maxwell equations is valid. In the reduced eddy current problem, these techniques are simplified to only the lattice, omitting the co-lattice. In this case, the inverse power flow problem is the inverse problem of the reduced eddy current problem. A commonly used lattice structure is the cuboid grid [7], which will be discussed in this section. However, the results for cuboid grids are generally applicable to most 3D lattices. We show that for a grid of size larger than $3 \times 3 \times 3$ nodes, our method requires only two measurements.

Let us denote the height, width, and depth of the grid network with the variables i, j, k. The number of nodes is

$$n = i \cdot j \cdot k$$

and the number of edges is

$$m = 3 \cdot i \cdot j \cdot k - i \cdot j - i \cdot k - j \cdot k.$$

Theorem 4. *In a grid network with $i, j, k \geq 3$, we need two measurements, with maximal independent solution sets $\mathscr{R}_1, \mathscr{R}_2$ to get a unique solution for the inverse problem.*

Proof. Since $i, j, k \geq 3$ we have:

$$i \cdot j \cdot k \geq i \cdot j + i \cdot k + j \cdot k$$

We evaluate the inequality (16) from Theorem 2 with $l = 2$ and get

$$\begin{aligned} & l \cdot (n-1) - (l-1) \cdot m \\ = & 2 \cdot (i \cdot j \cdot k - 1) - (3 \cdot i \cdot j \cdot k - i \cdot j - i \cdot k - j \cdot k) \\ \leq & 2 \cdot (i \cdot j \cdot k - 1) - 2 \cdot i \cdot j \cdot k \\ = & -2 \leq 0 \end{aligned}$$

Which proofs

$$\dim\left(\mathscr{R}_1 \cap \mathscr{R}_2\right) = 0,$$

such that only two measurements suffice to determine $\boldsymbol{R}$ uniquely. □

5 | Stability Analysis

The algorithm performs optimally for data sets devoid of measurement errors or noise. In this section, we examine the effects of measurement errors on the algorithm's performance. We performed simulations with randomly generated 3D cuboid grids whose boundary conductances were uniformly distributed between 0.2 and 2 S. On these networks, we used randomly generated external edge voltage sources, uniformly distributed between −1 and 1 V. Subsequently, the resulting edge currents were calculated. This process was repeated twice for each randomly generated network to obtain two sets of external edge voltage sources and corresponding edge currents. In order to simulate measurement errors, the edge currents were multiplied by random error factors with 2.5 %, 5 %, and 10 % error.

We have carried out simulations with different configurations of rectangular networks, external voltage sources, and measurement errors. In all these simulations, the results are similar. Therefore, we have decided to present the results of a 3D grid, since only two measurements are required to solve the problem, whereas, for example, three measurements are usually necessary for 2D grids.

We then calculated the edge resistances using only the correct external voltage sources and the resulting incorrect edge currents. We then compared the calculated edge resistances with the original edge resistances for each edge. For example, for a network with 1000 edges, a single simulation gives 1000 different results. For each result, we calculated the relative error, rounded it to the nearest percentage, and recorded it in a table. This was done for all errors except those exceeding 100 %, which were summarized in the last column. This entire procedure was repeated for numerous different networks.

We used 100 different networks, and for each simulation, an error of 2.5%, 5.0% and 10.0% was applied to the resulting edge currents. First, we observe from Figure 1 that the error of the calculated edge resistances grows proportionally with the percental measurement error. However, it also shows that for a high percentage of the edges, the calculated edge resistance exhibits a reasonable error. However, especially in the case of a percental error of 10 % and two measurements about 1% of the edges, the error exceeds 100%. Please note that for faulty input data, it is possible that the algorithm calculates negative resistances, which are then evaluated as errors with more than 100% deviation. These can be quickly identified as faulty. In the case of 10 % error, this affects 29% (0.31% total) of the edges evaluated with 100% deviation.

Generally spoken, to achieve more accurate results, one potential approach is to calculate the resistances using more than the two current measurements. The described algorithm can use

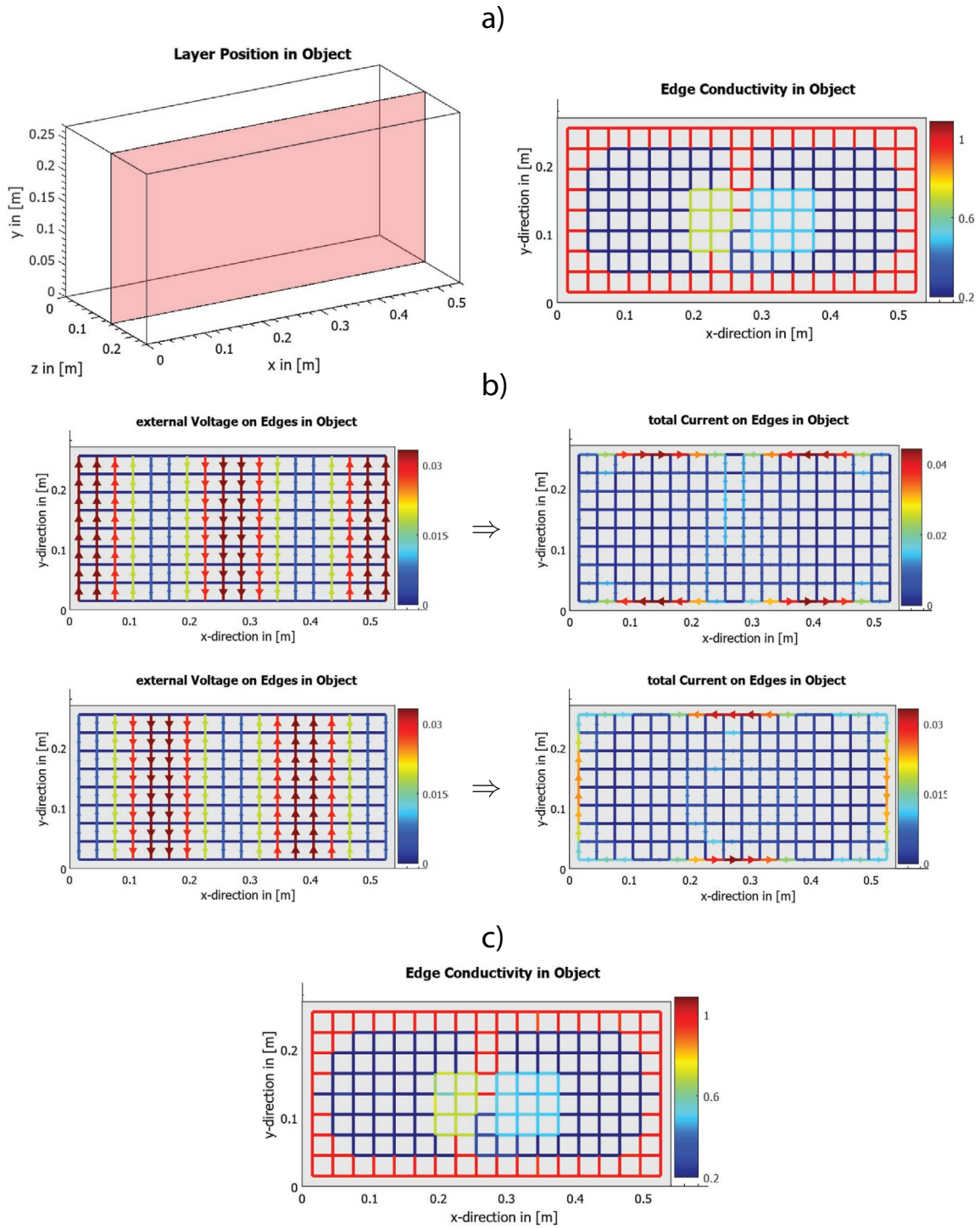

FIGURE 3 | Reconstruction in a 2D layer of a 3D cuboid grid with a current measurement error of 5%: (a) object layer position and original edge conductances; (b) two external voltages and two resulting currents; and (c) reconstructed edge conductances.

any number of measurements. The right column of Figure 1 shows the improvement of the calculated resistances when three instead of two measurements were simulated. For a direct comparison, we utilized the same 100 networks as in the previous figure, with two of the three measurements being identical to those used previously, and an additional third measurement included. The figure shows that the number of errors exceeding 100% has entirely disappeared for the cases of 2.5% and 5% current measurement errors.

A small but significant number of errors above 100% can still be seen in the histogram for an error of 10% even for a number of three measurements. Here, however, a fourth measurement leads to the desired result, which can be seen in Figure 2.

However, depending on the external voltage sources used, the network configuration, and the measurement error, the number of measurements required for reliable data may exceed 3. Still, it

will remain significantly smaller than the total number of network edges.

Finally, we provide an example within the MIT setting. Here, the electric field induced by an external harmonic magnetic field can be interpreted as external voltages applied to the edges of the network model. Additionally, at low frequencies of the harmonic magnetic field, the effect of the secondary magnetic field is minimal and does not significantly impact the primary field (i.e., we adhere to the magneto-quasi-static approximation). Consequently, the network model behaves as a resistive network, allowing the use of the presented calculation methods to solve the inverse problem. An example of such a calculation is shown in Figure 3. There, we consider the reconstruction of the edge conductances of a 3D cuboid grid with $17 \times 9 \times 8$ nodes, by showing one of its 2D sections. The 3D object is exposed to an external undulator field, as presented in [17, 18]. The measurement error for the currents is 5%.

6 | Conclusion

The introduced algorithm uniquely and exactly solves the nonlinear inverse power flow problem for any network with a maximum of three measurements; for the majority of 3D networks, even two measurements are sufficient. However, in the presence of measurement errors or noisy data, the algorithm may produce significant errors on individual network edges. By utilizing more than the required number of measurements, most of these errors can be mitigated.

Acknowledgments

This research was funded by the Federal State North Rhine-Westphalia, grant number 005-2105-0047, under the title "INDIGO-M." Open Access funding enabled and organized by Projekt DEAL.

Data Availability Statement

Research data are not shared.

References

1. Y. Yuan, S. H. Low, O. Ardakanian, and C. J. Tomlin, "Inverse Power Flow Problem," *IEEE Transactions on Control of Network Systems* 10, no. 1 (2023): 261–273.

2. C. W. Morgenstern, J. H. Morgenstern, R. Yang, and E. Cook, "Analyzing Accuracy of Inverse Power Flow From Noisy Edge Measurements," in *2022 IEEE Power & Energy Society Innovative Smart Grid Technologies Conference (ISGT)* (IEEE, 2022), 1–5.

3. S. Kim, O. Kwon, J. K. Seo, and J. R. Yoon, "On a Nonlinear Partial Differential Equation Arising in Magnetic Resonance Electrical Impedance Tomography," *SIAM Journal on Mathematical Analysis* 34, no. 3 (2002): 511–526.

4. J. K. Seo, J. R. Yoon, E. J. Woo, and O. Kwon, "Reconstruction of Conductivity and Current Density Images Using Only One Component of Magnetic Field Measurements," *IEEE Transactions on Biomedical Engineering* 50, no. 9 (2003): 1121–1124.

5. Y. Z. Ider, S. Onart, and W. R. Lionheart, "Uniqueness and Reconstruction in Magnetic Resonance–Electrical Impedance Tomography (MR–EIT)," *Physiological Measurement* 24, no. 2 (2003): 591.

6. Y. J. Kim, O. Kwon, J. K. Seo, and E. J. Woo, "Uniqueness and Convergence of Conductivity Image Reconstruction in Magnetic Resonance Electrical Impedance Tomography," *Inverse Problems* 19, no. 5 (2003): 1213–1225.

7. T. Schledewitz, M. Klein, and D. Rueter, "Magnetic Induction Tomography: Separation of the Ill-Posed and Non-Linear Inverse Problem Into a Series of Isolated and Less Demanding Subproblems," *Sensors* 23, no. 3 (2023): 1059.

8. P. Dimo, *Nodal Analysis of Power Systems* (Abacus Press, 1975).

9. Y. Tian, "The Dimension of Intersection of k Subspaces," *Missouri Journal of Mathematical Sciences* 14, no. 2 (2002): 92–95.

10. A. Korjenevsky and V. Cherepenin, "Magnetic Induction Tomography," *Radiotekhnika i Elektronika* 42 (1997): 506–512.

11. W. R. Purvis, R. C. Tozer, and I. L. Freeston, "Impedance Imaging Using Induced Currents," in *Proceedings of the Annual International Conference of the IEEE Engineering in Medicine and Biology Society*, 12 (IEEE, 1990), 114115.

12. J. M. Scaife, R. C. Tozer, and I. L. Freeston, "Real and Imaginary Impedance Images Using Induced Currents," in *Proceedings of the 12th Annual International Conference of the IEEE Engineering in Medicine and Biology Society*, 12 (IEEE, 1990), 116–117.

13. M. Clemens and T. Weiland, "Discrete Electromagnetism With the Finite Integration Technique," *Progress In Electromagnetics Research* 32 (2001): 65–87.

14. T. Weiland, "A Discretization Method for the Solution of Maxwell's Equations for Six-Component Fields," *Electronics and Communications AEU* 31, no. 3 (1977): 116–120.

15. E. Tonti, "On the Geometrical Structure of Electromagnetism," *Gravitation, Electromagnetism and Geometrical Structures* 281 (1995): 308.

16. E. Tonti, "Finite Formulation of the Electromagnetic Field," *Progress In Electromagnetics Research* 32 (2001): 1–44.

17. M. Klein, D. Erni, and D. Rueter, "Three-Dimensional Magnetic Induction Tomography: Improved Performance for the Center Regions Inside a Low Conductive and Voluminous Body," *Sensors* 20, no. 5 (2020): 1306.

18. M. Klein, D. Erni, and D. Rueter, "Three-Dimensional Magnetic Induction Tomography: Practical Implementation for Imaging Throughout the Depth of a Low Conductive and Voluminous Body," *Sensors* 21, no. 22 (2021): 7725.